AD 606050

[redacted]

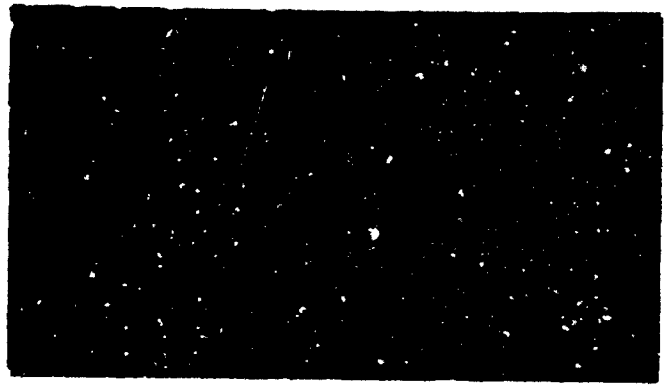

HYDRONAUTICS, incorporated
research in hydrodynamics

Research consulting and advanced engineering in the fields of NAVAL and INDUSTRIAL HYDRODYNAMICS. Offices and Laboratory in the Washington, D.C. area Pindell School Road Howard County Laurel Md.

HYDRONAUTICS, Incorporated

TECHNICAL REPORT 233-5

MECHANICAL PROPERTIES OF METALS AND THEIR CAVITATION DAMAGE RESISTANCE

By

A. Thiruvengadam
and
Sophia Waring

June 1964

Prepared Under

Office of Naval Research
Department of the Navy
Contract No. Nonr 3755(00)(FBM)
062-283

TABLE OF CONTENTS

LIST OF FIGURES

NOTATION

S_e^*	Estimated strain energy
T	Ultimate tensile strength
ϵ	Ultimate elongation
Y	Yield strength
S_e'	True strain energy
n	Strain hardening factor
T_f'	True fracture strength
ϵ_f	Elongation at fracture
I	Intensity of cavitation damage
r	Rate of volume loss
A_e	Area of erosion
S_e	Strain energy
r'	Correlation factor
a	Amplitude

SUMMARY

Detailed investigations with a magnetostriction apparatus were carried out to determine the cavitation damage resistance of eleven metals in distilled water at 80°F. The cavitation damage resistance is defined as the reciprocal of the rate of volume loss for a given metal. Among the mechanical properties investigated (ultimate tensile strength, yield strength, ultimate elongation, Brinell hardness, modulus of elasticity and strain-energy), the most significant property which characterizes the energy absorbing capacity of the metals, under the repeated, indenting loads due to the energy of cavitation bubble collapse in the steady state zone, was found to be the fracture strain energy of the metals. The strain energy is defined as the area of the stress-strain diagram up to fracture. The correlation between the strain energy and the reciprocal of the rate of volume loss leads directly to the estimation of the intensity of cavitation damage; this intensity varies as the square of the displacement amplitude of the specimen. All these conclusions are limited to the steady state zone of damage.

INTRODUCTION

Since the work of Parsons (1) in 1919 and Föttinger (2) in 1926, there have been many attempts to characterize the cavitation damage resistance of materials by a single, common mechanical property. Although Honegger (3), in 1927, did not find any correlation between hardness and erosion resistance, Gardner (4),

in 1932, found that the hardness of a metal was the principal property in determining the resistance to erosion. Many more references may be cited to bring out similar controversies with regard to other mechanical properties such as yield strength, ultimate tensile strength, ultimate elongation and modulus of elasticity. One can get a clear picture of the magnitude of the conflicts in this area from some of the excellent review articles in the technical literature (5,6,7).

These controversies are a result of an inadequate understanding of the mechanism of cavitation damage. Recent advances in this direction have made it possible to rationalize some of the conflicts, and to propose a mechanical property that most significantly characterizes the cavitation damage resistance of metals in the absence of corrosion. It is the purpose of this paper to develop the logic behind such an argument, and to present recent substantiating experimental evidence.

One of the basic parameters involved in the testing of materials for cavitation damage resistance is the test duration. The rate of loss of material depends upon the test duration itself even though every other test parameter is maintained precisely constant. Recent analysis showed that there exist four zones of damage with respect to testing time. They are:

1. Incubation Zone
2. Accumulation Zone
3. Attenuation Zone
4. Steady State Zone

A detailed discussion of these zones appears elsewhere (14). All the results and conclusions presented herein are limited to the steady state zone of damage in which the rate of damage does not change with time.

MECHANISM OF CAVITATION DAMAGE

It is now generally established that the bubble collapse energy produces indentations on the metal as shown in Figure 1. The indentations may be produced on the material either by the impingement of jets or by shock waves. The evidence in support of these methods of dent formation is abundant in the literature (8,9,10,11,12). In the absence of corrosion, it is quite reasonable to proceed on the assumption that these dents, formed by mechanical means, are the main cause of fracture and loss of metal.

When such repeated, indenting forces or blows act upon a metallic surface, one of the following events may occur depending upon the intensity of impact:

(i) There may not be any permanent deformation;

(ii) The metal may deform after a certain number of repetitive blows;

(iii) A permanent deformation may develop at the onset of the first blow; and

(iv) The metal may 'splash' and 'wash-out' on the first blow itself or after a certain number of repetitions.

These possibilities can be readily understood from Figure 2 which shows schematically the variation of the internal friction of metals with strain amplitude in the case of repeated loadings. In the case of cavitation damage, it is reasonable to assume, for the sake of the present argument, that the energy of collapse for a given frequency, amplitude, and liquid varies in a statistical manner as shown by the hypothetical distribution in Figure 3. As the strain amplitude is increased, the mean strain may increase, the mean number of bubbles possessing adequate energy of collapse to produce this strain may increase, or both of these possibilities may occur. In any case, the response of a metal to a given strain can be qualitatively explained by an equivalent indentation fatigue diagram as shown in Figure 4. Accordingly, the response of a metal to a cavitation damage test is dependent upon the order of magnitude of the strain. In Figure 4 three regions have been designated to point out the possible material responses to indentation events discussed previously. Photographs of the metallic surfaces which exhibited the response of each region are also shown.

With the above physical picture in mind, let us pose the question: What is the characteristic property of a metal that controls the eroded volume as a result of this mechanical process? Obviously this property is the energy absorbing capacity per unit volume of the metal up to fracture when subjected to the repeated overlapping indentations. At the present state of knowledge, there is no way to determine this quantity exactly. For this reason, several investigators have tried to correlate this quantity with most of the commonly known mechanical properties of metals.

Our superficial intuition initially suggests that the hardness of the surface may be of utmost importance. However, when the physical meaning of hardness is examined critically, we find that indentation hardness is essentially a measure of the yield stress of the material (13). It does not represent the full measure of the energy required for fracture because it neglects the elongation of the material up to its ultimate strength. Similar arguments can be advanced against other mechanical properties such as yield stress, ultimate stress and others. An earlier attempt to correlate the area of the stress-strain diagram up to fracture and the cavitation damage rate proved to be encouraging (12). The present investigation is an extension of this attempt in a more detailed manner and confirms the earlier results.

EXPERIMENTAL FACILITY AND TECHNIQUE

The HYDRONAUTICS, Incorporated Magnetostriction Apparatus was used for these investigations. The details of the equipment and the experimental procedure are outlined in Reference 14. A double cylinder velocity transformer replaced the exponential horn. In Figure 5 are shown the essential test parameters of the magnetostriction apparatus. Simple flat specimens were tested in distilled water at 27°C (approximately).

RESULTS AND DISCUSSION

Metals Tested and Their Mechanical Properties

The following metals were tested.

Group 1.

(i) 1100-O Aluminum
(ii) Cast Iron
(iii) Molybdenum
(iv) 410 Stainless Steel
(v) 304-L Stainless Steel

Group 2.

(i) 1100-F Aluminum
(ii) 2024-T4 Aluminum
(iii) 1020 Mild Steel
(iv) Tobin Bronze
(v) Monel
(vi) 316 Stainless Steel

For the materials listed under Group 1, the mechanical properties were obtained from the literature. The typical values in the references varied over a range as shown in Table 1. These values are available only for the common properties such as yield strength, ultimate strength, ultimate elongation, Brinell hardness and modulus of elasticity. Even typical stress-strain diagrams are a rarity in the literature for these metals. Further, it should be realized that these properties vary from heat to heat for the same material. However, a preliminary attempt was

made to correlate the cavitation damage resistance with these mechanical properties. For this purpose, the strain energy was roughly estimated from the following relationship

$$S_e^* = (T + Y)\frac{\epsilon}{2} \qquad [1]$$

where

S_e^* is the estimated strain energy,

T is the ultimate tensile strength,

ϵ is the ultimate elongation, and

Y is the yield strength.

This relationship was used since the values of T, Y and ϵ were readily available and gives an approximate value of the area of the stress-strain diagram, assuming it to be a trapezoid. Among the properties considered in this preliminary analysis, the best correlation was obtained with this estimated strain energy as shown in Figure 6. Since T, Y and ϵ vary over a wide range, the estimated value of the strain energy also varies over a range; this range is shown in Figure 6 by a solid line for each material, while the mean value is shown by a solid circle. This analysis revealed the need for additional test data.

The second group of six metals was selected for actual tests and detailed analysis. The engineering stress-strain diagrams were obtained from the same bar stock of material from which the cavitation test specimens were machined. The stress-strain

diagrams for these six materials are given in Figure 7. These data were obtained according to the Federal Test Method Standard TT-, No. 151a with half an inch diameter tensile specimens of two inch gauge length (15). The true stress-strain diagrams for the six metals are shown in Figure 8. The strain energy was computed by the following three methods:

1. Area of the true stress-strain diagram given by the relationship

$$S_e' = \left(\frac{1}{1+n}\right) T_f' \epsilon_f \qquad [2]$$

where

S_e' is the true strain energy,

n is the strain hardening factor,

T_f' is the true fracture strength, and

ϵ_f is the elongation at fracture.

2. Area of the engineering stress-strain diagram obtained by direct measurement.

3. An approximate estimation according to Equation [1].

The reason for employing these three methods is to determine the percentage deviation among the three strain energy values.

The mechanical properties of the second group of six metals, obtained by actual tests, are listed in Table 2. However, the Brinell hardness values shown in this table are typical values

reported in the literature. It can be seen that the strain energy values computed by the above three methods agree closely, within ±10 percent, with the true strain energy as the standard.

Cavitation Damage Resistance

All of these metals were tested for their cavitation damage resistance according to the procedures outlined in detail in Reference 14. Essentially, the procedure is to test each of the metals under a given set of experimental conditions through the four zones of damage, namely, incubation zone, accumulation zone, attenuation zone and steady state zone. It is of interest to note that all the metals which were tested exhibited these zones. The specimen that had reached the steady state zone was used to obtain the relationship between the rate of volume loss and the displacement amplitude as shown in Figure 9. The reciprocal of the rate of volume loss is defined as the cavitation damage resistance of a material. The cavitation damage resistance at a given amplitude (2×10^{-3}cm) in the steady state zone was plotted against the various mechanical properties of the metals as shown in Figures 10 through 15. The mechanical properties considered here are strain energy, ultimate tensile strength, yield strength, Brinell hardness, ultimate elongation and modulus of elasticity. Both groups of metals have been included for this correlation. The values of linear correlation factor for each of the above mechanical properties are tabulated below.

Mechanical Property	Correlation Factor
Strain Energy	0.91
Ultimate Strength	0.79
Yield Strength	0.65*
Brinell Hardness	0.51
Modulus of Elasticity	0.49
Ultimate Elongation	0.48

The correlation factor, r', for two variables, x and y, is calculated from the following formula:

$$r' = \frac{n\epsilon_{xy} - \epsilon_x \epsilon_y}{\sqrt{\left[n\epsilon_x^2 - (\epsilon_x)^2\right]\left[n\epsilon_y^2 - (\epsilon_y)^2\right]}}$$

where

n is the number of points in an x, y plane.

---

* This is based on ten sample points since the yield strength for cast iron is not available.

This analysis clearly shows that the most significant linear correlation is obtained with the strain energy of the material. It follows from this result that the energy absorbing capacity of a metal characterizing the cavitation damage resistance is largely determined by the strain energy.

Limitations

1. This analysis is confined to six common properties of metals. It is not implied that there is no other property more significant than strain energy.

2. This analysis is limited to the steady state zone. In the earlier zones, the interaction of the strain hardening exponent and the surface roughness will have to be taken into account.

3. No superposition of a corrosive environment is considered in this analysis. The interaction of a corrosive environment on the fatigue properties of metals is important.

Intensity of Cavitation Damage

One of the immediate uses of this correlation is to estimate the intensity of cavitation damage as a function of displacement amplitude. The intensity has been defined as the power absorbed per unit area of the material (16) and is given by

$$I = \frac{r.S_e}{A_e} \qquad [3]$$

where

I is the intensity of cavitation,

r is the rate of volume loss,

A_e is the area of erosion, and

S_e is the strain energy.

It can be seen that the intensity of cavitation damage for a given amplitude is given by the reciprocal of the slope of the line in Figure 10 divided by the area of erosion. The best fit lines by the least square method for each amplitude are shown in Figure 16. The intensity, thus computed, varies as the square of the amplitude for the experimental conditions in the steady state zone (Figure 17).

CONCLUSIONS

The following conclusions are drawn as a result of these investigations

1. Among the mechanical properties investigated to characterize the energy absorbing capacity of metals under the repeated indentations produced by cavitation damage, the most significant correlation is obtained with the strain energy of the metal, where the strain energy is defined as the area of the stress-strain diagram up to fracture in a simple tensile test. This conclusion is limited to the steady state zone of damage in a non-corrosive environment.

2. The above relationship leads directly to the estimation of the intensity of cavitation damage. According to this estimate the intensity varies as the square of the displacement amplitude in the steady state zone under the present experimental conditions.

ACKNOWLEDGMENTS

This investigation was supported by the Office of Naval Research, Department of the Navy, Contract No. Nonr 3755(00)(FBM) NR 062-293. Many useful discussions with Mr. H. S. Preiser during the course of this work are gratefully acknowledged.

REFERENCES

1. Parsons, C. A. and Cook, S. S., "Investigations into the Causes of Corrosion or Erosion of Propellers," Engineering, Volume 107, pp. 515-519, 1919.

2. Föettinger, H., "Untersuchungen ueber Kavitation und Korrosion bei Turbinen, Turbo-pumpes und Propellers in Hydraulisobe Probleme," (Berlin) V.D.I. Verlag, pp. 14-64, 1926.

3. Honegger, E., Concerning Erosion Experiments, Brown Boveri Review, 14, pp. 74-95, 1927.

4. Gardner, O., "The Erosion of Steam Turbine Blades," Engineer, Lond., Vol. 153, pp. 146-205, 1932.

5. Nowotny, H., "Werstoff Zerstoorung durk Kavitation," V.D.I. Verlag, Gimbh, Berlin, 1942, English Translation as ORA Report No. 03424-15-I, Nuclear Engineering Department, University of Michigan, 1962.

6. Godfrey, D. J., "Cavitation Erosion" - A Review of Present Knowledge, Report Prepared for the Inter-Services Metallurgical Research Council Corrosion and Electro-deposition Committee, Ministry of Supply (England) September, 1957.

7. Eisenberg, Phillip, "Cavitation Damage," HYDRONAUTICS, Incorporated Technical Report 233-1, December 1963.

8. Boetcher, H. M., "Failures of Metals Due to Cavitation Under Experimental Conditions," Trans. ASME, Vol. 58, pp. 355-360, 1936.

9. Wheeler, W. H., "Mechanism of Cavitation Erosion," Proc. Symposium on Cavitation in Hydrodynamics, National Physical Laboratory, Paper No. 21, H.M.S.O. (London) Publication 1956.

10. Naude, C. F., and Ellis, A. T., "On the Mechanism of Cavitation Damage by Nonhemispherical Cavities Collapsing in Contact with a Solid Boundary," ASME Paper No. 61 - Hyd - 8, January 30, 1961.

11. Bowden, F. P., and Brunton, J. H., "The Deformation of Solids by Liquid Impact at Supersonic Speeds," Proc. Roy. Soc. A., Vol. 263, pp. 433-450, October 10, 1961.

12. Thiruvengadam, A., "A Unified Theory of Cavitation Damage," Trans. ASME, Vol. 85, pp. 365-377, September 1963.

13. Tabor, D., "The Physical Meaning of Indentation and Scratch Hardness," British Journal of Applied Physics, Vol. 7, pp. 159-166, May 1956.

14. Thiruvengadam, A., and Preiser, H. S., "On Testing Materials for Cavitation Damage Resistance," HYDRONAUTICS, Incorporated Technical Report 233-3, December 1963.

15. Metals; Test Methods, Supplement A Fed. Test Method Std. No. 151, July 19, 1956, Notice 1, May 6, 1959.

16. Thiruvengadam, A., "A Comparative Evaluation of Cavitation Damage Test Devices," HYDRONAUTICS, Incorporated Technical Report 233-2, November 1963 (See also Symposium on Cavitation Research Facilities and Techniques, ASME, May 1964, pp. 157-164.)

TABLE 1

Mechanical Properties of Five Metals from Literature

	Ultimate Strength dynes/cm²*		Yield Strength dynes/cm²		Ultimate Elongation		Brinell Hardne		Modulus of Elasticity dynes/cm²
	Max.	Min.	Max.	Min.	Max.	Min.	Max.	Min.	
1100-O-Aluminum	89.6×10^7	-	34.4×10^7	-	45	35	23	-	68.9×10^{10}
Cast Iron	310×10^7	138×10^7	-	-	10	5	265	110	103.3×10^{10}
Molybdenum	792×10^7	469×10^7	689×10^7	310×10^7	42	5	250	200	317×10^{10}
410 Stainless Steel	827×10^7	413×10^7	620×10^7	241×10^7	30	15	300	150	193×10^{10}
304-L Stainless Steel	661×10^7	482×10^7	655×10^7	172×10^7	60	25	280	150	200×10^{10}

* $\frac{\text{dynes}}{\text{sq cm}} = 1.45 \times 10^{-5}$ lbs/sq in.

TABLE 2 - Mechanical Properties of Six Metals from Actual Tensile Tests

Material	Units	Modulus of Elasticity	Yield Strength	Ultimate Tensile Strength	Hardness BHN	Density g/cm³	True Ultimate Tensile Strength	Strain Hardening Factor	Ultimate Elongation %	True Ultimate Elongation %	True Strain Energy	Engineering Strain Energy	Estimated Strain Energy
316 Stainless Steel	psi	25×10^6	68×10^3	91.4×10^3	160	7.98	12.6×10^4	0.16	44	36	39.0×10^6	37.0×10^3	35.0×10^6
	dynes/cm²	172×10^{10}	469×10^7	630×10^7			86.8×10^8				269×10^7	255×10^7	241×10^7
Monel	psi	26×10^6	77.9×10^3	97.9×10^3	125	8.84	11.2×10^4	0.088	27	24	24.7×10^6	23.7×10^3	23.7×10^6
	dynes/cm²	179×10^{10}	537×10^7	675×10^7			77.2×10^8				170×10^7	163×10^7	163×10^7
1020 Mild Steel	psi	24×10^6	91.0×10^3	112.6×10^3	130	7.85	14.6×10^4	0.13	12	11.5	14.9×10^6	12.5×10^3	12.2×10^6
	dynes/cm²	165×10^{10}	627×10^7	776×10^7			101×10^8				103×10^7	86.1×10^7	84.1×10^7
Tobin Bronze	psi	12×10^6	57.7×10^3	72.0×10^3	125	8.41	8.3×10^4	0.102	26	23.5	17.6×10^6	17.8×10^3	16.9×10^6
	dynes/cm²	82.7×10^{10}	398×10^7	496×10^7			57.2×10^8				121×10^7	123×10^7	116×10^7
2024 Aluminum	psi	10×10^6	50.4×10^3	70.6×10^3	120	2.70	8.1×10^4	0.143	21.5	19.5	13.8×10^6	13.7×10^3	13.0×10^6
	dynes/cm²	68.9×10^{10}	347×10^7	486×10^7			55.8×10^8				95×10^7	94×10^7	89.6×10^7
1100-F Aluminum	psi	9×10^6	19.8×10^3	22.3×10^3	42	2.70	2.6×10^4	0.065	19.5	17.2	4.2×10^6	3.2×10^3	4.1×10^6
	dynes/cm²	62.0×10^{10}	136×10^7	154×10^7			17.9×10^8				28.9×10^7	22.0×10^7	28.2×10^7

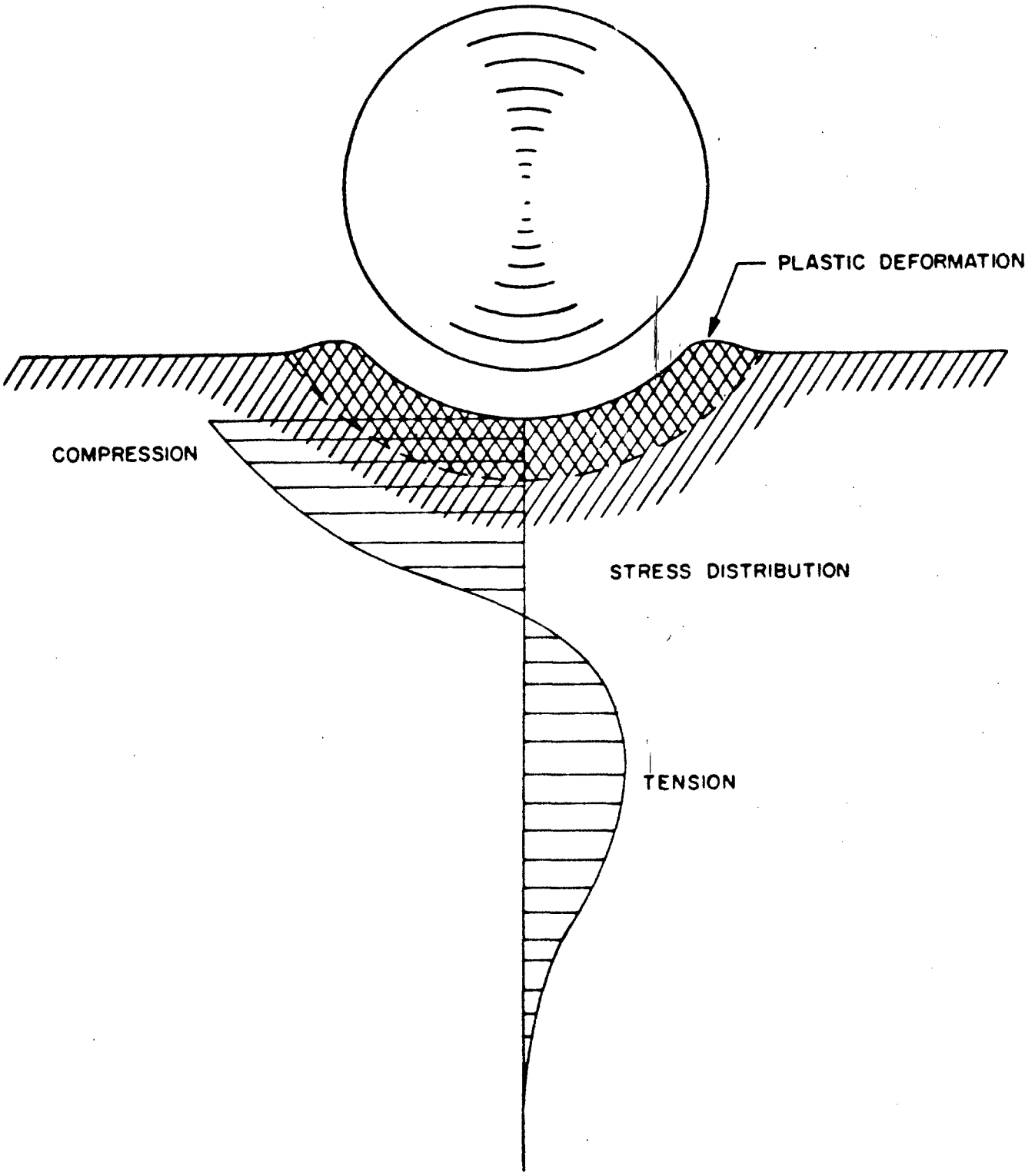

FIGURE 1 -DEFINITION SKETCH FOR DEFORMATION DUE TO CAVITATION BUBBLE COLLAPSE

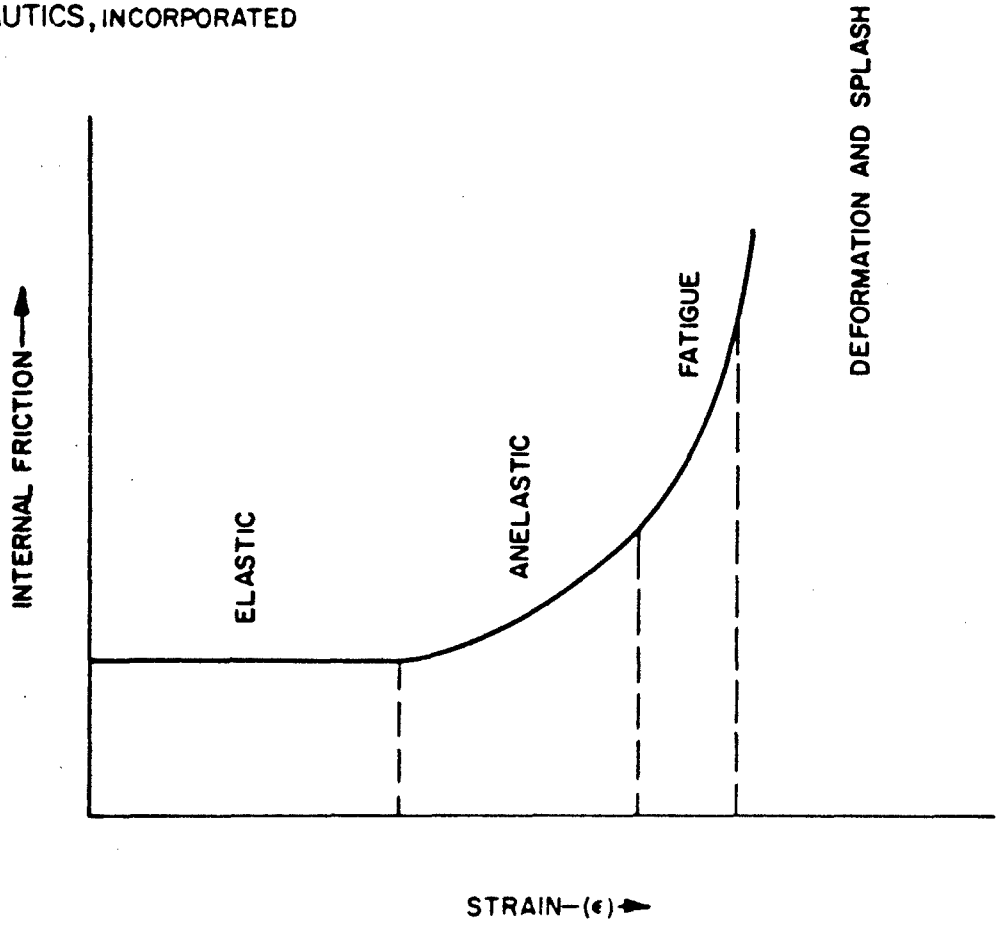

FIGURE 2—SCHEMATIC REPRESENTATION OF THE RESPONSE OF METALS TO REPEATED STRAINING

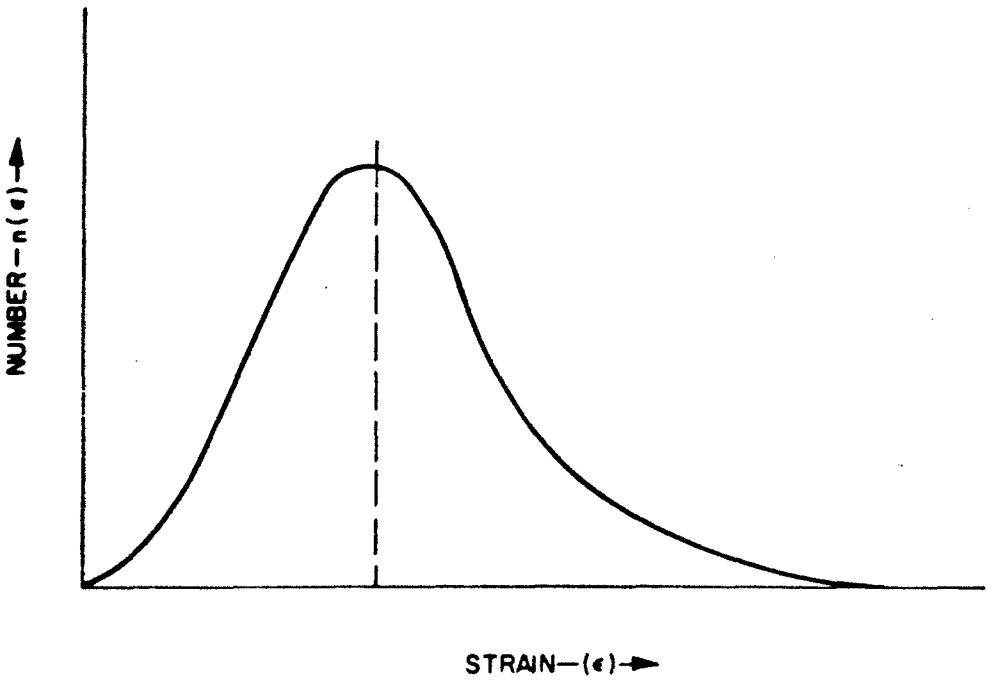

FIGURE 3 - HYPOTHETICAL DISTRIBUTION OF STRAINS CAUSED BY THE COLLAPSE OF BUBBLES IN A CAVITY CLOUD

AMPLITUDE: 2.0 X 10^{-3} CM
FREQUENCY: 14 KCS
LIQUID DISTILLED WATER: @ 27° C

REGION 1

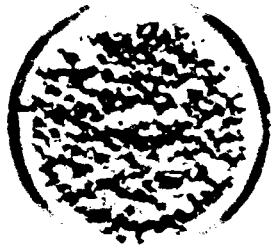

1100-F ALUMINUM
TEST TIME=0.5 HRS

REGION 2

316 STAINLESS STEEL
TEST TIME=55 HRS.

REGION 3

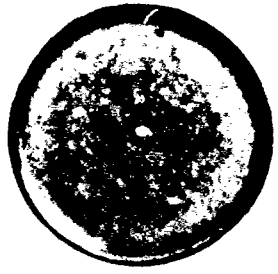

TENALON
TEST TIME=<3 HRS.

ENERGY OF INDENTATION

NUMBER OF CYCLES

HYDRONAUTICS, INCORPORATED

f = 14 KCS
a = 0.7 X 10^{-3}-3.0 X 10^{-3}CM
2r = 1.59 CM
d ≃ 0.3 CM
H ≃ 8.0 CM
D ≃ 7.0 CM
LIQUID: DISTILLED WATER @ 27°C

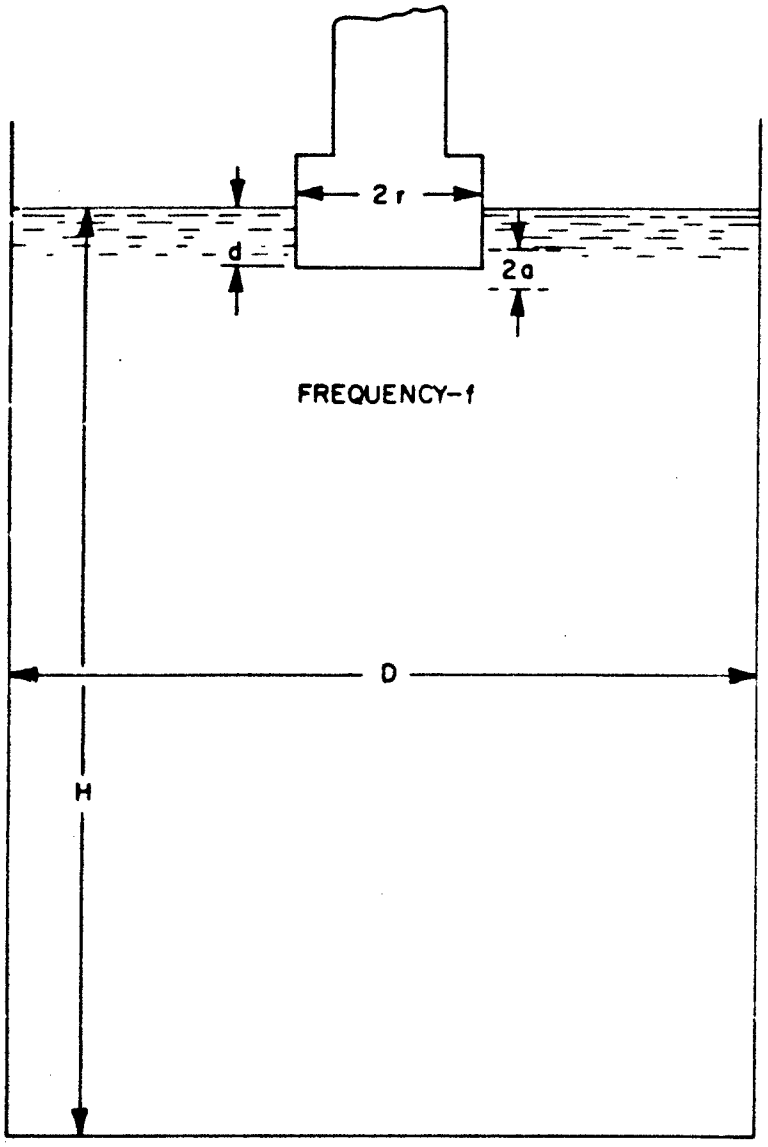

FIGURE 5-DEFINITION SKETCH OF THE MAGNETOSTRICTION DEVICE

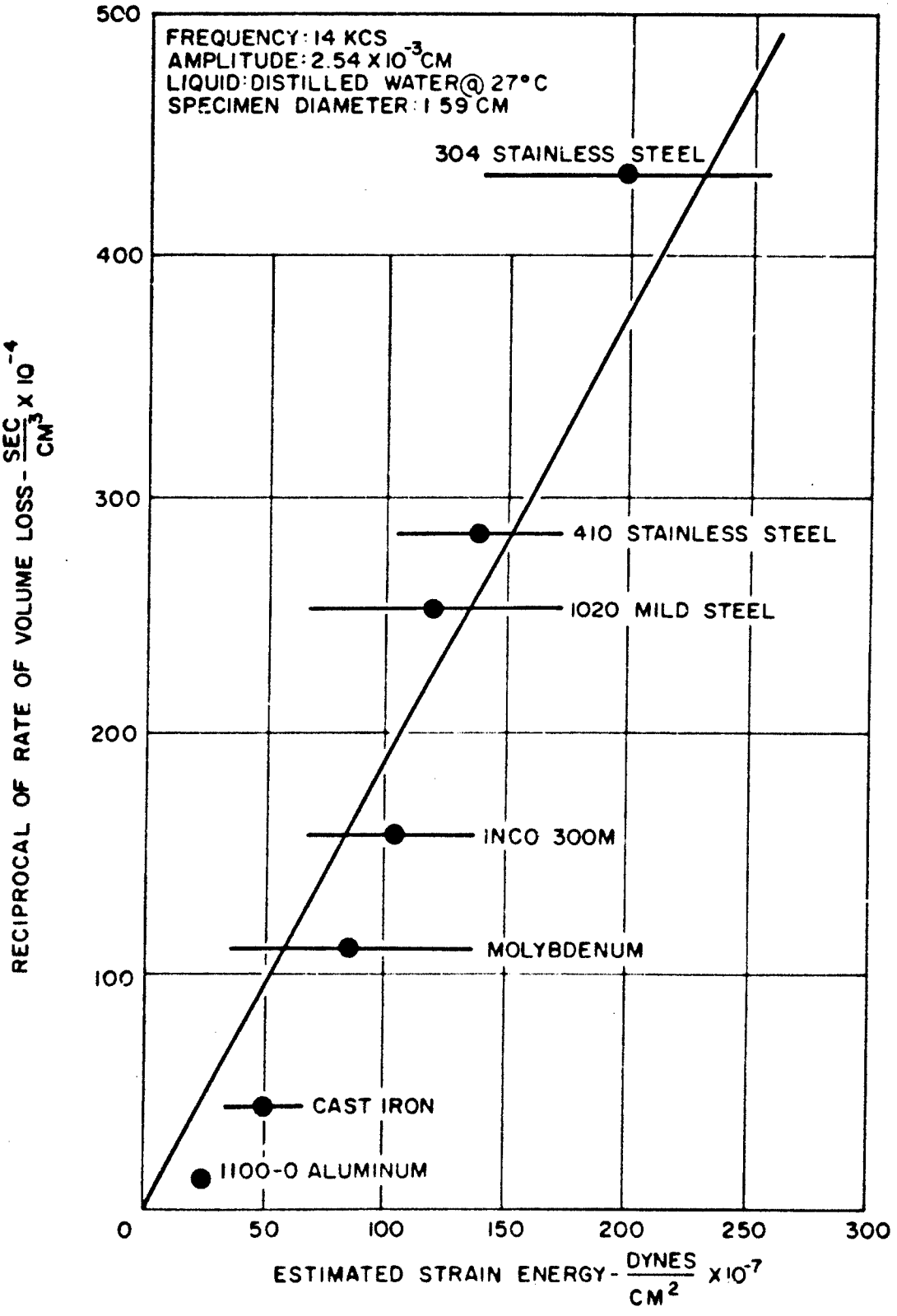

FIGURE 6 - CORRELATION BETWEEN ESTIMATED STRAIN ENERGY AND RECIPROCAL OF RATE OF VOLUME LOSS

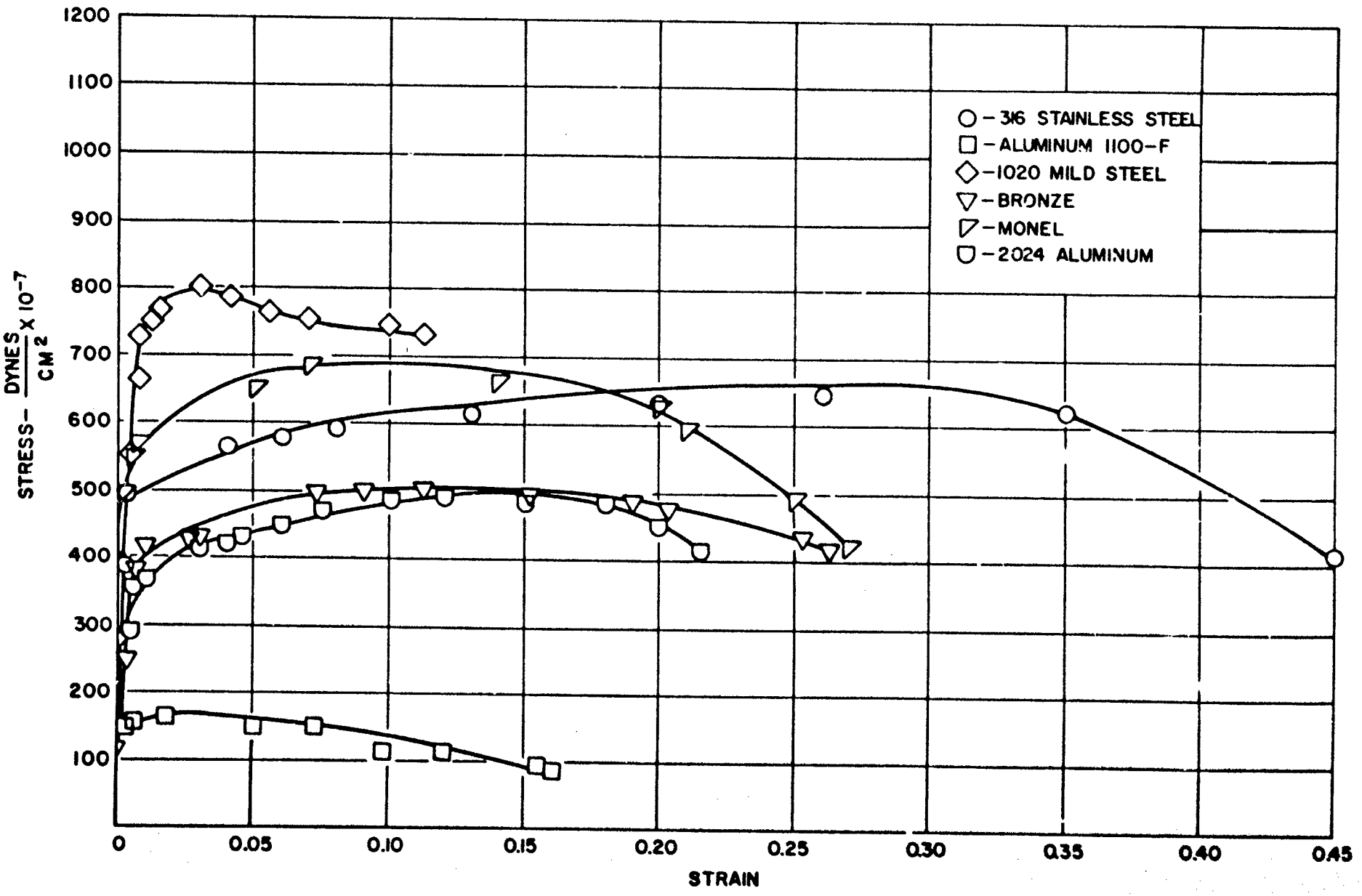

FIGURE 7-ENGINEERING STRESS-STRAIN DIAGRAMS FOR SIX METALS

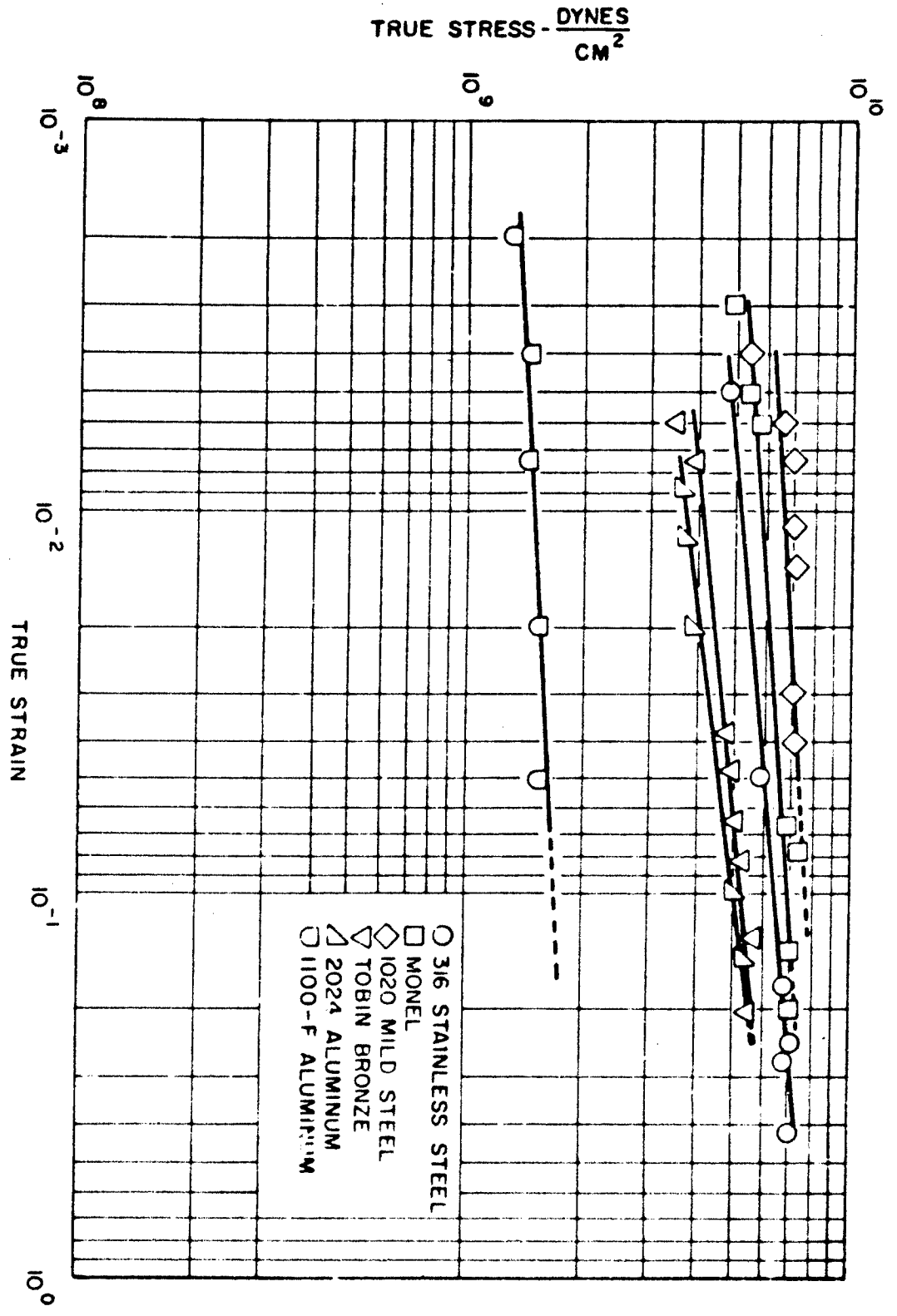
TRUE STRESS - DYNES/CM²
10⁸
10⁹
10¹⁰
10⁻³
10⁻²
10⁻¹
10⁰
TRUE STRAIN
316 STAINLESS STEEL
MONEL
1020 MILD STEEL
TOBIN BRONZE
2024 ALUMINUM
1100-F ALUMINUM

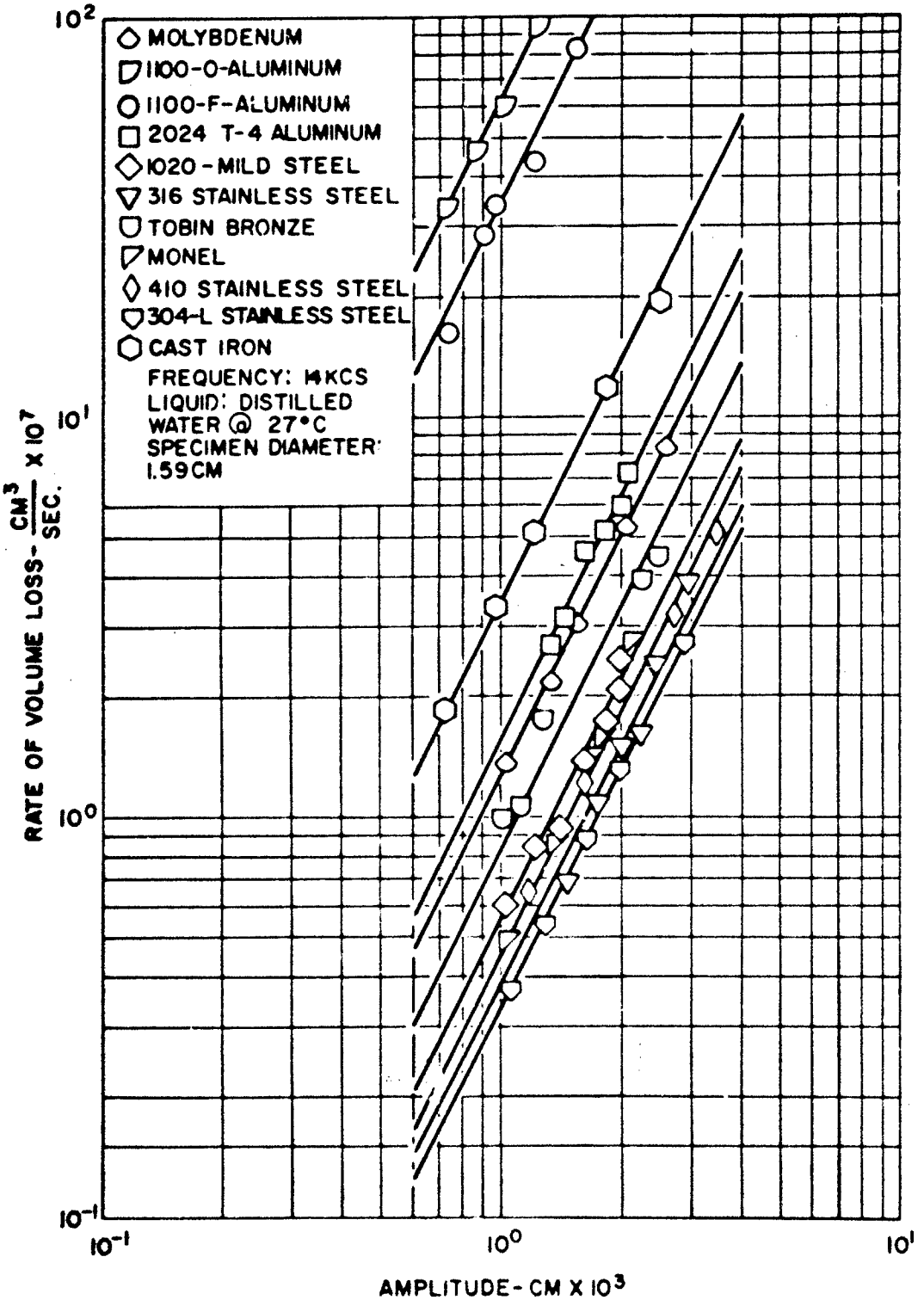

FIGURE 9-EFFECT OF AMPLITUDE ON DAMAGE RATE FOR ELEVEN METALS

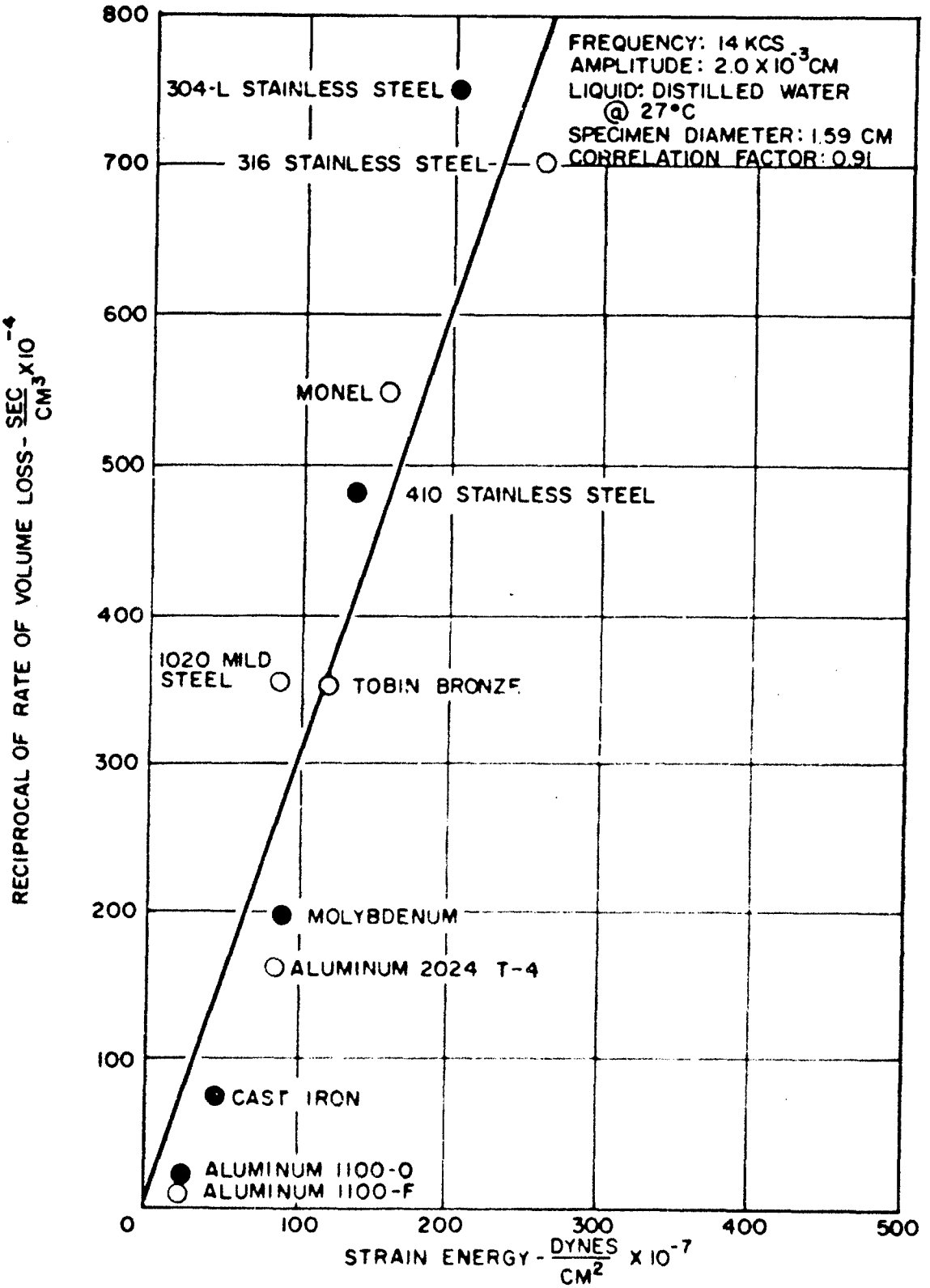

FIGURE 10-CORRELATION BETWEEN STRAIN ENERGY AND RECIPROCIAL OF RATE OF VOLUME LOSS

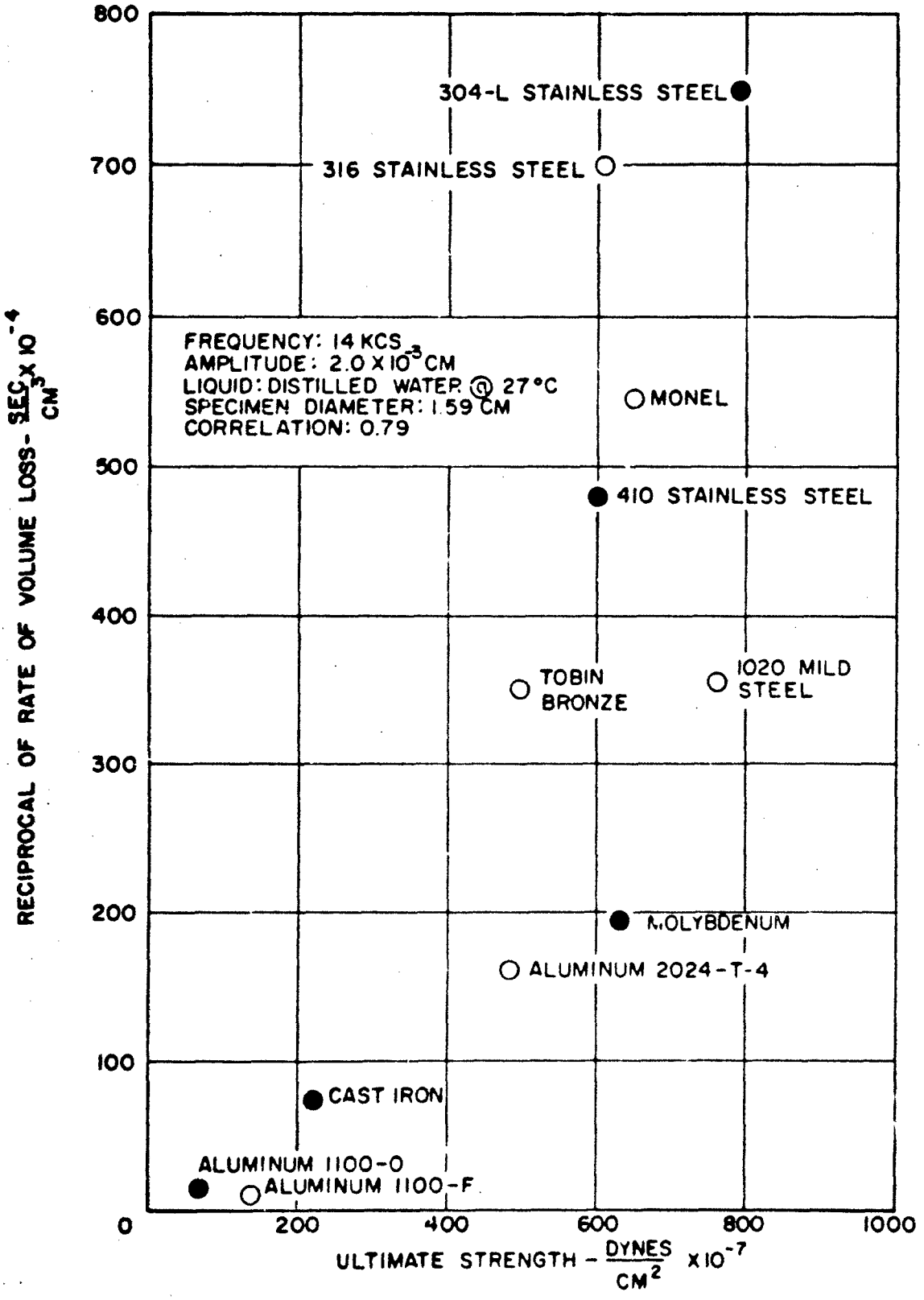

FIGURE 11 -CORRELATION BETWEEN ULTIMATE STRENGTH AND RECIPROCAL OF RATE OF VOLUME LOSS

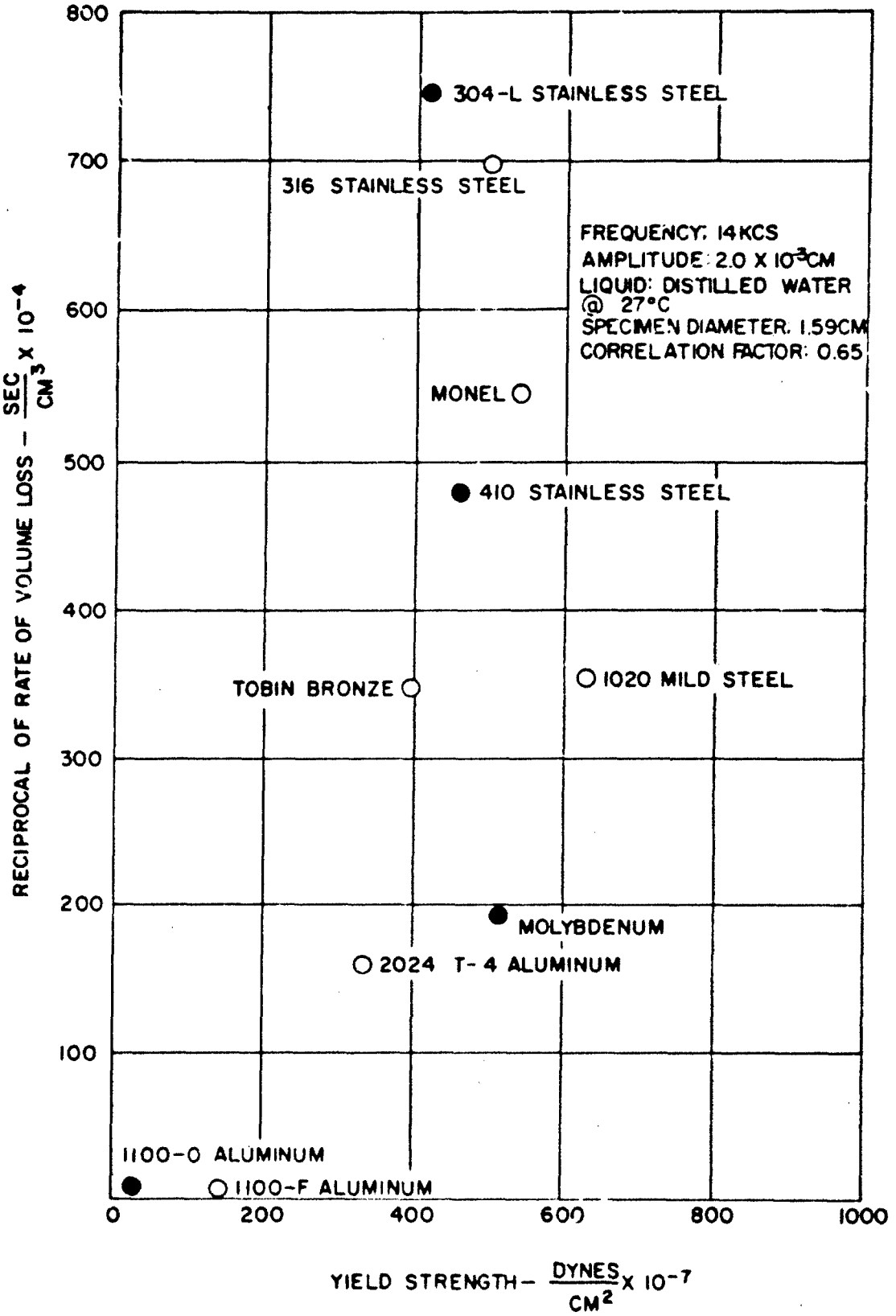

FIGURE 12-CORRELATION BETWEEN YIELD STRENGTH AND RECIPROCAL OF RATE OF VOLUME LOSS

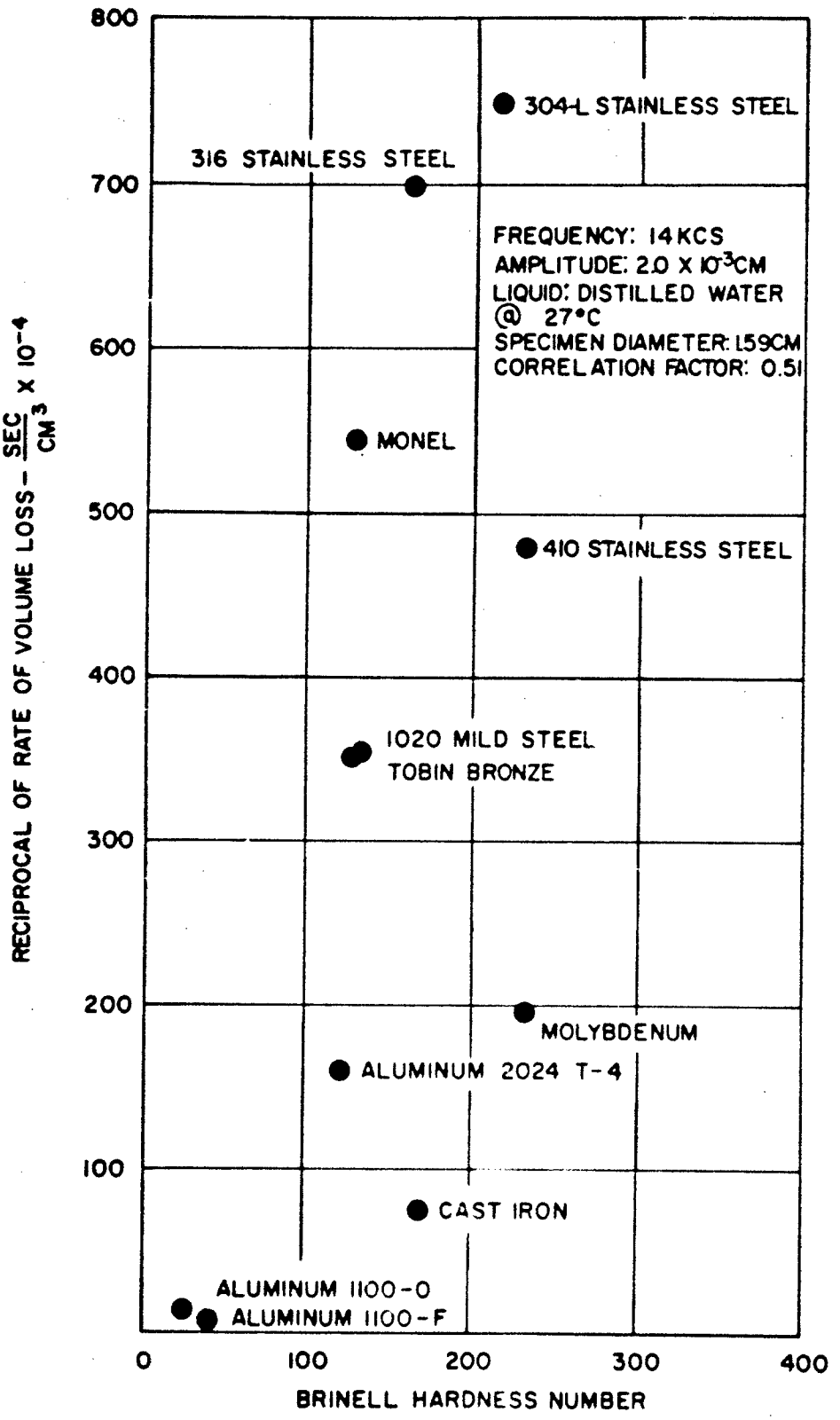

FIGURE 13-CORRELATION BETWEEN BRINELL HARDNESS AND RECIPROCAL OF RATE OF VOLUME LOSS

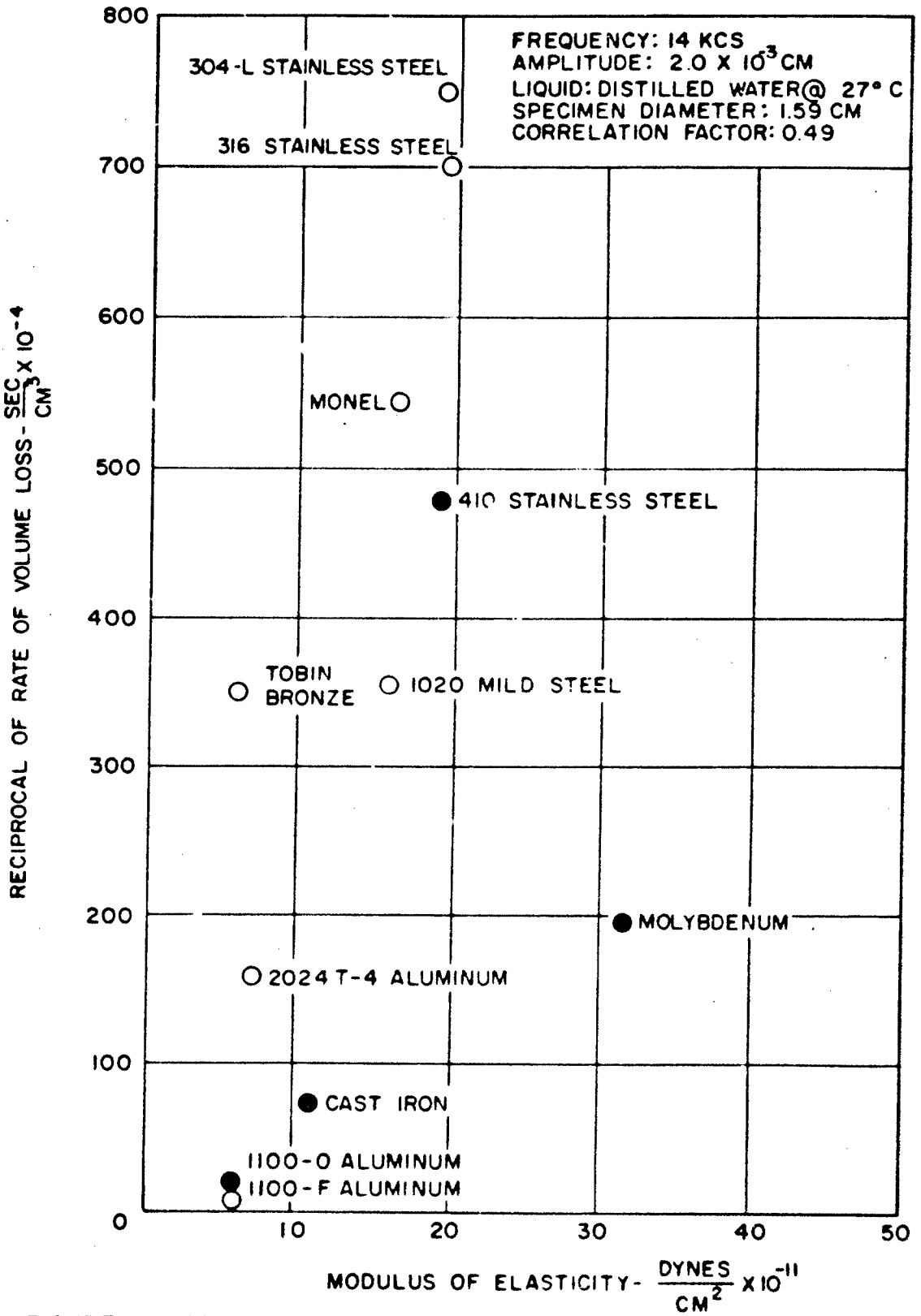

FIGURE 14 - CORRELATION BETWEEN MODULUS OF ELASTICITY AND RECIPROCAL OF RATE OF VOLUME LOSS

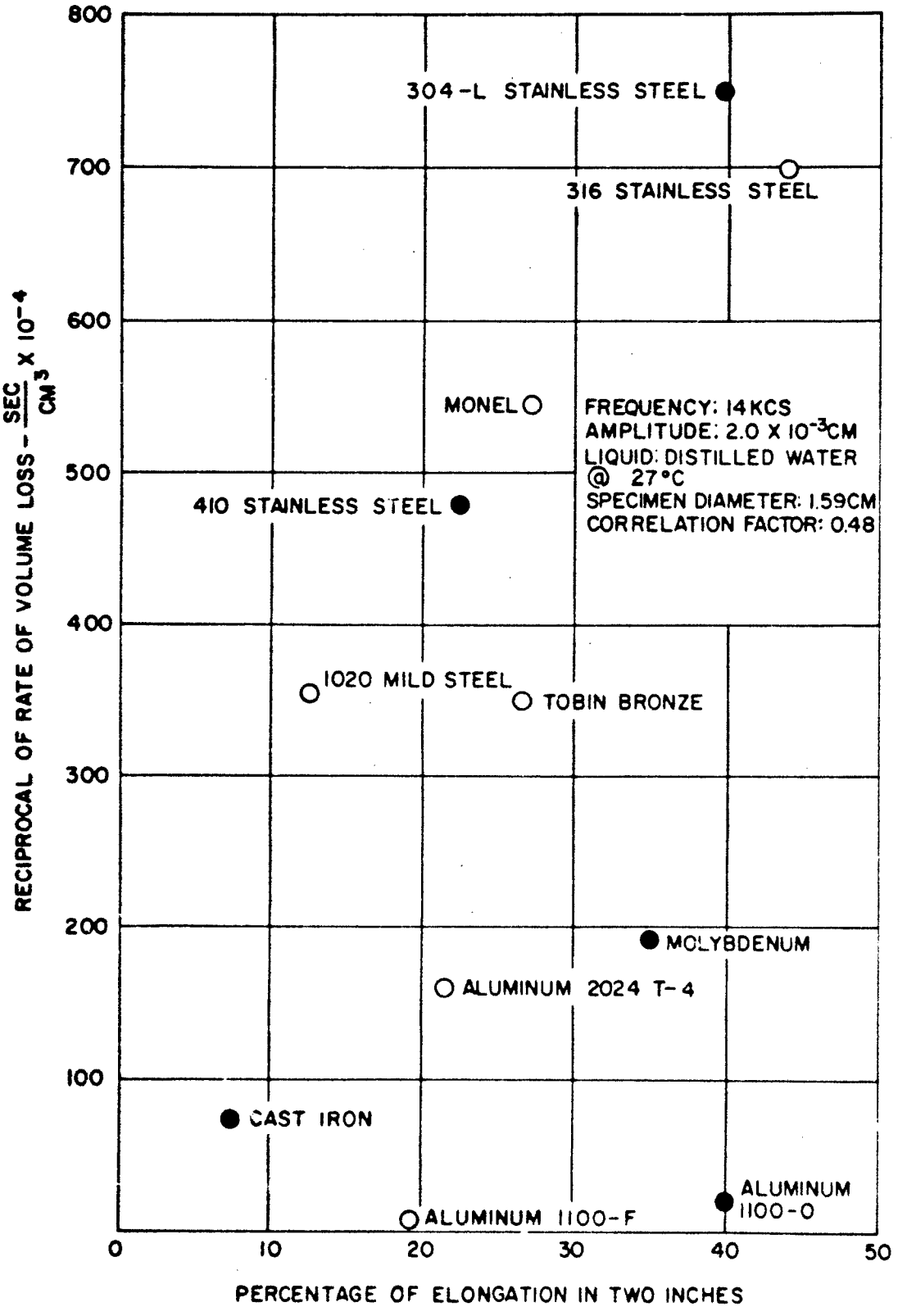

FIGURE 15–CORRELATION BETWEEN ULTIMATE ELONGATION AND RECIPROCAL OF RATE OF VOLUME LOSS

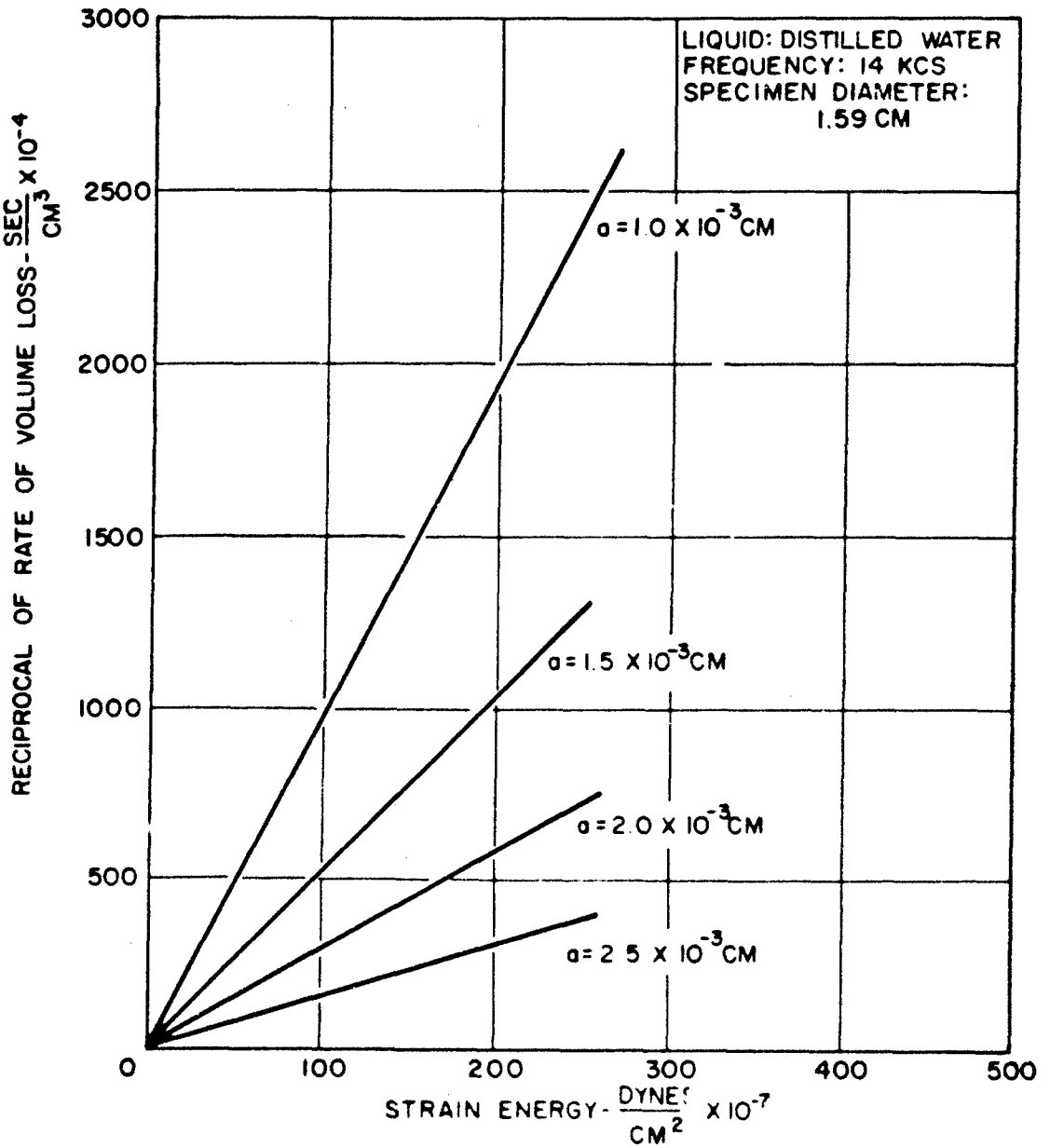

FIGURE 16-RELATIONSHIP BETWEEN STRAIN ENERGY AND RECIPROCAL OF RATE OF VOLUME LOSS AT VARIOUS AMPLITUDES

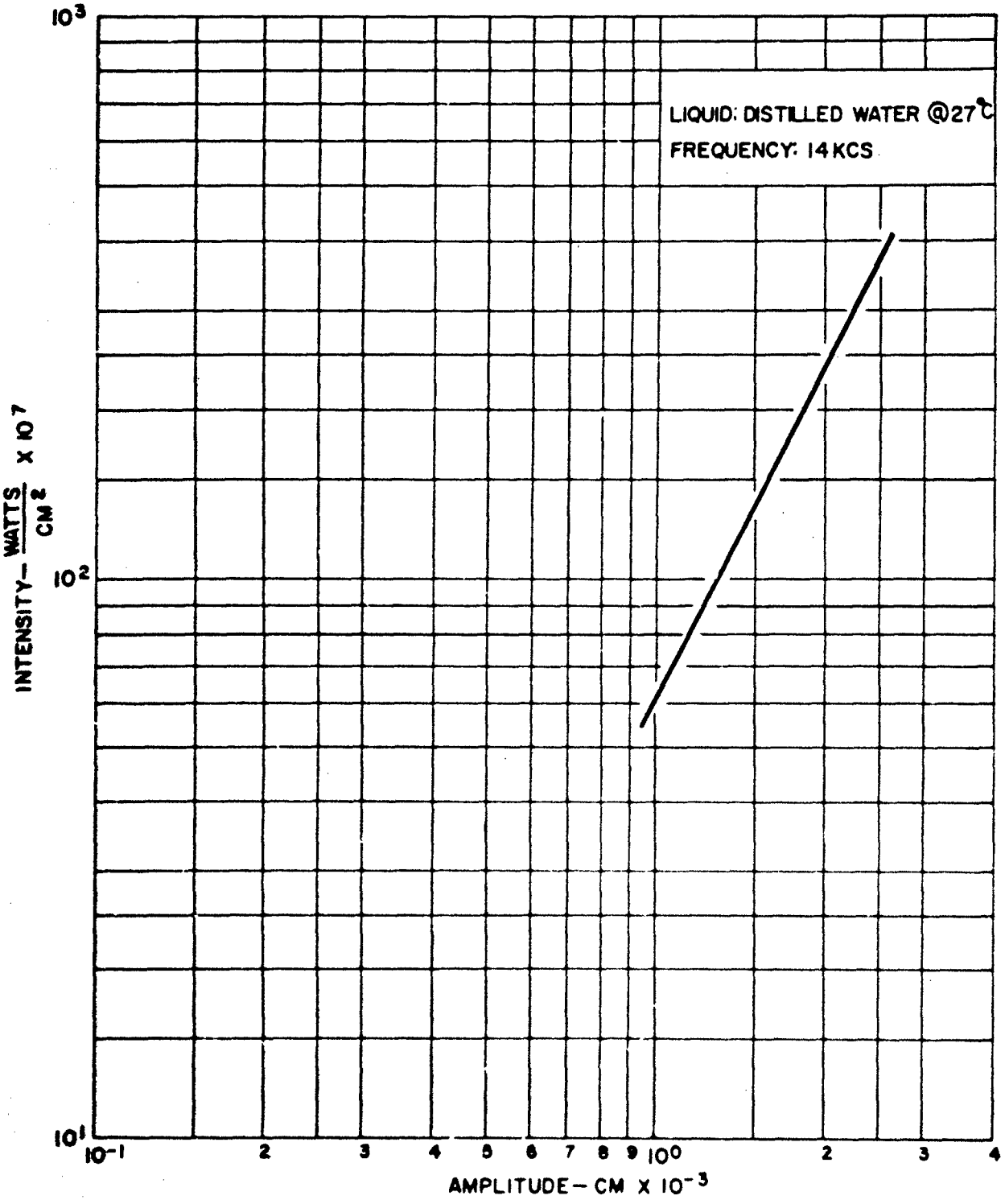

FIGURE 17-EFFECT OF DISPLACEMENT AMPLITUDE ON OUTPUT INTENSITY

HYDRONAUTICS, Incorporated

DISTRIBUTION LIST
(Contract Nonr 3755(00))

Chief of Naval Research
Department of the Navy
Washington 25, D. C.
Attn: Codes 438 — 3
Code 461 — 1
463 — 1
429 — 1

Commanding Officer
Office of Naval Research
Branch Office
495 Summer Street
Boston 10, Massachusetts — 1

Commanding Officer
Office of Naval Research
Branch Office
230 N. Michigan Avenue
Chicago 1, Illinois — 1

Commanding Officer
Office of Naval Research
Branch Office
207 West 24th Street
New York 11, New York — 1

Commanding Officer
Office of Naval Research
Branch Office
Navy No. 100, Box 39
Fleet Post Office
New York, New York — 25

Commanding Officer
Office of Naval Research
Branch Office
1030 East Green Street
Pasadena 1, California — 1

Commanding Officer
Office of Naval Research
Branch Office
1000 Geary Street
San Francisco 9, California — 1

Director
U. S. Naval Research Laboratory
Washington 25, D. C.
Attn: Codes 2000 — 1
2020 — 1
2027 — 6

Chief, Bureau of Ships
Department of the Navy
Washington 25, D. C.
Attn: Codes 300 — 1
305 — 1
335 — 1
341 — 1
342A — 1
345 — 1
421 — 1
440 — 1
442 — 1
634A — 1
Attn: Code 634(B.Taylor) — 1
Code 634(L. Birnbaum) — 1

Chief, Bureau of Naval Weapons
Department of the Navy
Washington 25, D. C.
Attn: Codes R — 1
R-12 — 1
RR — 1
RRRE — 1
RU — 1
RUTO — 1

Chief, Bureau of Yards and Docks
Department of the Navy
Washington 25, D. C.
Attn: Codes D-202 1
D-400 1
D-500 1

Commanding Officer and Director
David Taylor Model Basin
Washington 7, D. C.
Attn: Codes 142 1
500 1
513 1
521 1
526 1
550 1
563 1
589 1
Dr. M. Strasberg (901) 1

Commander
U. S. Naval Ordnance Laboratory
Silver Spring, Maryland
Attn: Dr. A. May 1
Desk DA 1
Desk HL 1
Desk DR 1

Commander
U. S. Naval Ordnance Test Station
China Lake, California
Attn: Codes 5014 1
4032 1
753 1

Hydrographer
U. S. Navy Hydrographic Office
Washington 25, D. C. 1

Commander
U. S. Naval Ordnance Test Statio
Pasadena Annex
3202 E. Foothill Boulevard
Pasadena 8, California
Attn: Mr. J.W. Hoyt 1
Research Division 1
P508 1
P804 1
P807 1
P80962 (Library) 1
Mr. J.W. Hicks 1

Superintendent
U. S. Naval Academy
Annapolis, Maryland
Attn: Library 1

Commanding Officer and Director
U. S. Navy Marine Engineering
Laboratory
Annapolis, Maryland 21402
Attn: Code 750 1

Commander
U. S. Naval Weapons Lab.
Dahlgren, Virginia
Attn: Tech. Library Div. 1
Computation and Exterior
Ballistics Laboratory
(Dr. Hershey) 1

Commanding Officer
NROTC and Naval Administrative
Unit
Massachusetts Institute of Tech.
Cambridge 39, Massachusetts 1

Commanding Officer and Director
U.S.Underwater Sound Laboratory
Fort Trumbull
New London, Connecticut
Attn: Technical Library 1

Commanding Officer and Director
U. S. Navy Mine Defense Laboratory
Panama City, Florida 1

Superintendent
U. S. Naval Postgraduate School
Monterrey, California
Attn: Library 1

Commanding Officer and Director
U. S. Naval Electronic Laboratory
San Diego 52, California
Attn: Code 4223 1

Commanding Officer and Director
U. S. Naval Civil Engineering Lab.
Port Hueneme, California 1

New York Naval Shipyard
Material Laboratory
Brooklyn 1, New York
Attn: Mr. C.K. Chatten
Code 949 1

Commander
Norfolk Naval Shipyard
Portsmouth, Virginia 1

Commander
New York Naval Shipyard
U. S. Naval Base
Brooklyn, New York 1

Commander
Boston Naval Shipyard
Boston 29, Massachusetts 1

Commander
Philadelphia Naval Shipyard
U. S. Naval Base
Philadelphia 12, Penn. 1

Commander
Portsmouth Naval Shipyard
Portsmouth, New Hampshire
Attn: Design Division 1

Commander
Charleston Naval Shipyard
U. S. Naval Base
Charleston, South Carolina 1

Commanding Officer
U. S. Naval Underwater
Ordnance Station
Newport, Rhode Island
Attn: Research Division 1

Commander
Long Beach Naval Shipyard
Long Beach 2, California 1

Commander
Pearl Harbor Naval Shipyard
Navy No. 128, Fleet Post Office
San Francisco, California 1

Commander
San Francisco Naval Shipyard
San Francisco 24, California 1

Shipyard Technical Library
Code 303TL, Bldg. 746
Mare Island Naval Shipyard
Vallejo, California 1

Superintendent
U. S. Merchant Marine Academy
Kings Point, Long Island,
New York
Attn: Dept. of Engr. 1

Commandant, U. S. Coast Guard
1300 E. Street, N. W.
Washington, D. C. 1

Beach Erosion Board
U. S. Army Corps of Engineers
Washington 25, D. C. 1

Commanding Officer
U. S. Army Research Office
Box CM, Duke Station
Durham, North Carolina 1

Commander
Hdqs. U.S. Army Transportation
Research and Development Command
Transportation Corps
Fort Eustis, Virginia 1

Director
U. S. Army Engineering Research
and Development Laboratories
Fort Belvoir, Virginia
Attn: Tech. Documents Center 1

Office of Technical Services
Department of Commerce
Washington 25, D. C. 1

Defense Documentation Center
Cameron Station
Alexandria, Virginia 10

Maritime Administration
441 G. Street, N. W.
Washington 25, D. C.
Attn: Coordinator of Research 1
Div. of Ship Design 1

Fluid Mechanics Section
National Bureau of Standards
Washington 25, D. C.
Attn: Dr. G.B. Schubauer 1

U. S. Atomic Energy Commission
Technical Information Service
Extension, P. O. Box 62
Oak Ridge, Tennessee 1

Scientific and Technical
Information Facility
Attn: NASA Representative
P. O. Box 5700
Bethesda, Maryland 20014 1

Director
Langley Research Center
National Aeronautics and
Space Administration
Langley Field, Virginia 1

Director
Ames Research Laboratory
National Aeronautics and
Space Administration
Moffett Field, California 1

National Aeronautics and
Space Administration
Lewis Research Center
21000 Brookpark Road
Cleveland, Ohio 44135
Attn: Director 1
Mr. Cavour H. Hauser 1
Mr. James P. Couch 1

Director
Engineering Science Division
National Science Foundation
Washington, D. C. 1

Commander
Air Force Cambridge Research
Center, 230 Albany Street,
Cambridge 39, Massachusetts
Attn. Geophysical Research
Library 1

Air Force Office of Scientific
Research, Mechanics Division
Washington 25, D. C. 1

National Research Council
Montreal Road
Ottawa 2, Canada
Attn: Mr. E.S. Turner 1

Engineering Societies Library
29 West 39th Street
New York 18, New York 1

Society of Naval Architects and
Marine Engineers
74 Trinity Place
New York 6, New York 1

Webb Institute of Naval
Architecture
Glen Cove, Long Island, New York
Attn: Prof. E.V. Lewis 1
Technical Library 1

The Johns Hopkins University
Baltimore 18, Maryland
Attn: Prof S. Corrsin 1
Prof. F.H. Clauser 1
Prof. O.M. Phillips 1

Director
Applied Physics Laboratory
The Johns Hopkins University
8621 Georgia Avenue
Silver Spring, Maryland 1

New York State University
Maritime College
Engineering Department
Fort Schuyler, New York
Attn: Prof. J. J. Foody 1

California Institute of Tech.
Pasadena 4, California
Attn: Hydrodynamics Lab. 1
Prof. T. Y. Wu 1
Prof. A. Ellis 1
Prof. A. Acosta 1
Prof. M. Plesset 1

University of California
Berkeley 4, California
Attn: Department of Engineering
Prof. H. A. Schade 1
Prof. J. Johnson 1
Prof. J.V. Wehausen 1
Prof. E.V. Laitone 1
Prof. P. Lieber 1
Prof. M. Holt 1

University of California
Los Angeles, California
Attn: Prof. R.W. Leonard 1
Prof. A. Powell 1

Director
Scripps Institution of Oceanography
University of California
La Jolla, California 1

Iowa Institute of Hydraulic Research
State University of Iowa
Iowa City, Iowa
Attn: Prof. H. Rouse 1
Prof. L. Landweber 1
Prof. P. G. Hubbard 1

Harvard University
Cambridge 38, Massachusetts
Attn: Prof. G. Birkhoff 1
Prof. S. Goldstein 1

University of Michigan
Ann Arbor, Michigan
Attn: Engineering Research Institute 1
Prof. F.G. Hammitt 1

Director
Ordnance Research Laboratory
Pennsylvania State University
University Park, Pennsylvania
Attn: Dr. G.F. Wislicenus 1

Director
St. Anthony Falls Hydraulic Lab.
University of Minnesota
Minneapolis 14, Minnesota
Attn: Mr. J.N. Wetzel 1
Prof. B. Silberman 1
Prof. L.G. Straub 1

Massachusetts Institute of Technology
Cambridge 39, Massachusetts
Attn: Prof. P. Mandel 1
Prof. M.A. Abkowitz 1

Institute for Fluid Mechanics and Applied Mathematics
University of Maryland
College Park, Maryland
Attn: Prof. J.M. Burgers 1

Cornell Aeronautical Laboratory
Buffalo 21, New York
Attn: Mr. W.F. Milliken, Jr 1

Brown University
Providence 12, Rhode Island
Attn: Dr. R.E. Meyer 1
Dr. W.H. Reid 1

Stevens Institute of Technology
Davidson Laboratory
Hoboken, New Jersey
Attn: Mr. D. Savitsky 1
Mr. J.P. Breslin 1
Dr. D.N. Hu 1
Dr. S.J. Lukasik 1

Director
Woods Hole Oceanographic Inst.
Woods Hole, Massachusetts 1

Director
Alden Hydraulic Laboratory
Worcester Polytechnic Institute
Worcester, Massachusetts 1

Stanford University
Stanford, California
Attn: Dr. Byrne Perry
(Dept. of Civil Engr) 1
Prof. E.Y. Hsu
(Dept. of Civil Engr.) 1
Dr. S. Kline
(Dept. of Mech. Engr.) 1

Dr. E.R.G. Eckert
Mechanical Engineering Department
University of Minnesota
Minneapolis, Minnesota 55455 1

Department of Theoretical and Applied Mechanics
College of Engineering
University of Illinois
Urbana, Illinois
Attn: Dr. J.M. Robertson 1

Department of Mathematics
Rensselaer Polytechnic Institute
Troy, New York
Attn: Prof. P.C. DiPrima 1

Southwest Research Institute
8500 Culebra Road
San Antonio 6, Texas
Attn: Dr. H.N. Abramson 1

Department of Aeronautical Engr.
University of Colorado
Boulder, Colorado
Attn: Prof. M.S. Uberoi 1

Courant Institute
New York University
New York, New York
Attn: Prof. P. Garabedian 1

Institut fur Schiffbau der
Universitat Hamburg
Lammersieth 90
Hamburg 33, Germany
Attn: Prof. O. Grim 1
Prof. K. Wieghardt 1

Max-Planck Institut fur
Stromungsforschung
Bottingerstrasse 6-8
Gottingen, Germany
Attn: Dr. H. Reichardt,Dir. 1

Professor Dr.-Ing. S. Schuster
Baudirector
Versuchsanstalt fur Wasserbau
und Schiffbau
Berlin, Germany 1

Netherlands Ship Model Basin
Wageningen, The Netherlands
Attn: Ir. R. Wereldsma 1
Dr. J.B. Van Manen 1

Mitsubishi Shipbuilding and
Engineering Company
Nagasaki, Japan
Attn: Dr. K. Taniguchi 1

Mr. W.R. Wiberg, Chief
Marine Performance Staff
The Boeing Company
Aero-Space Division
P. O. Box 3707
Seattle 24, Washington 1

Mr. William P. Carl
Grumman Aircraft Corporation
Bethpage, L.I., New York 1

Grumman Aircraft Corporation
Bethpage, L.I. New York
Attn: Engineering Library,
Plant 5 1
Mr. Leo Geyer 1

Mr. G. W. Paper
ASW and Ocean Systems Dept.
Lockheed Aircraft Corporation
Burbank, California 1

Dr. A. Ritter
Therm Advanced Research Div.
Therm, Incorporated
Ithaca, New York 1

HYDRONAUTICS, Incorporated
Pindell School Road
Howard County
Laurel, Maryland
Attn: Mr. P. Eisenberg 1
(President)
Mr. M.P. Tulin
(Vice President) 1

Dr. J. Kotik
Technical Research Group, Inc.
Route 110
Melville, New York 1

AiResearch Manufacturing Company
9851-9951 Sepulveda Boulevard
Los Angeles 45, California
Attn: Blaine R. Parkin 1

Hydrodynamics Laboratory
Convair
San Diego 12, California
Attn: Mr. H.E. Brooke 1
Mr. R.H. Oversmith 1

Baker Manufacturing Company
Evansville, Wisconsin 1

Gibbs and Cox, Inc.
21 West Street
New York 16, New York 1

Electric Boat Division
General Dynamics Corporation
Groton, Connecticut
Attn: Mr. R. McCandliss 1

Mr. A Grindell
Oak Ridge National Laboratory
Oak Ridge, Tennessee 1

ITT Research Institute
10 W. 35th Street
Chicago 16, Illinois 1

Missile Development Division
North American Aviation, Inc.
Downey, California
Attn: Dr.E. R. Van Driest 1

National Physical Laboratory
Teddington, Middlesex, England
Attn: Head Aerodynamics Div.
Mr. A. Silverleaf 1

Aerojet General Corporation
6352 N. Irwindale Avenue
Azusa, California
Attn: Mr. C.A. Gongwer 1

Astropower, Inc.
2121 Paularino Avenue
Newport Beach, California
Attn: R. D. Bowerman 1

Transportation Technical
Research Institute
No. 1057-1-Chome
Mejiro-machi, Toshima-ku
Tokyo-to, Japan 1

Oceanics, Incorporated
Plainview, Long Island, N.Y.
Attn: Dr. Paul Kaplan 1

Director, Special Projects Offi
Department of the Navy
Washington 25, D. C.
Attn: Code SP-001 1

National Academy of Sciences
National Research Council
Committee on Undersea Warfare
2101 Constitution Avenue
Washington 25, D. C. 1

Dr. Harvey Brooks
School of Applied Sciences
Harvard University
Cambridge, Massachusetts 1